

## THE REDUCTION OF RIGID-BODY RESPONSE OF STING SUPPORTED MODELS AT HIGH ANGLES OF INCIDENCE

by

D. G. Mabey  
 B. L. Welsh  
 C. R. Pyne

Royal Aerospace Establishment  
 Bedford MK41 6AE, UK

ABSTRACT

During an investigation of scale effects at high Reynolds number on a swept wing model, dangerous bending oscillations occurred in a vertical plane at a Mach number of 0.50 in the incidence range from 27°-29°. In addition dangerous yawing oscillations occurred in a horizontal plane above an incidence of about 35°. These tests were reviewed to establish wider implications for tests on wind tunnel models of combat aircraft at high angles of incidence and at the high kinetic pressures needed for Reynolds numbers close to full scale values.

The review suggested that similar dangerous motions might occur (possibly without prior warning) on other models at high angles of incidence unless special preventive measures were taken. An internal tuned damper and balance bump stops were installed in the model to limit the responses. The bump stops also prevented the moment limits of the strain gauge balance from being exceeded.

1 INTRODUCTION

Current combat aircraft in flight at high angles of incidence (say  $\alpha = 20-30^\circ$ ) encounter a wide range of unsteady handling problems, such as wing rock, wing drop or nose slice (Fig 1a), some of which may be addressed by 'catastrophe theory'(1). All these flight problems are due to flow separation which cause rigid body motions at relatively low aerodynamic frequency parameters (say  $\nu = 2\pi f\bar{c}/U$  from 0.03-0.09). These rigid body motions are usually accompanied by large responses in structural modes (buffeting)(2) occurring at frequency parameters typically an order of magnitude higher ( $\nu$  from 0.3-0.9). Both types of problem may become more severe on the next generation of combat aircraft, designed to fly at even higher angles of incidence (say 30 to 60°). The flow separations exciting these rigid body motions may be subject to large scale effects, and hence there is a new requirement to test models of advanced combat aircraft at high angles of incidence combined with high kinetic pressures.

Such wind tunnel test programmes may be restricted because models generally have low frequency, rigid body modes on the balance or sting mounting, (typically in heave, pitch sideslip and yaw) in the same range of frequency parameter as the troublesome aircraft rigid body motions. Hence low frequency motions in these modes must be expected at high angles of incidence. At best, the possibility of severe buffeting in rigid body modes must be considered (Fig 1b). The level of this buffeting at high angles of

incidence is likely to be much higher than that due to the low level of flow unsteadiness in the wind tunnel(3), and will require an increase in measurement time to acquire accurate time-averaged measurements(4). At worst, the possibility of single degree of freedom flutter cannot be excluded (Fig 1c). Although this flutter may be amplitude limited, the model amplitudes might be sufficiently large to break the balance or cause structural failures at the high kinetic pressures required to generate high Reynolds numbers.

The risk of failures may be reduced by a number of changes in model design and test procedures discussed here. The process is illustrated by some brief measurements on a model that encountered serious vibration problems at high angles of incidence. This model has four adverse aerodynamic features (Fig 2): the square fuselage shape, the absence of a fin, the absence of a canard or a fuselage strake to improve the wing flow and the use of a wing with an uncambered leading edge, unsuited to high angles of incidence. In addition, transition was free on both the fuselage and the wing, which, according to previous experience in many dynamic tests, would enhance the coupling between the flow and the model motion(5). Although this model was unrepresentative of a realistic design, it was considered that its behaviour at high angles of incidence might indicate the behaviour of a realistic design, eg with transitional boundary layers at transonic speeds.

Despite these adverse aerodynamic features, significant reductions in rigid body response were obtained by two interim changes in the model structural dynamics (Fig 3). These changes were the use of an internal tuned damper to reduce the amplitude of the vertical bending mode at 6.7 Hz (Fig 3a) and the use of bump stops between the model and the sting to limit the amplitude in the yawing mode at 13.5 Hz to less than 0.5° (Fig 3b) so that the balance limits (different for the vertical bending and the yawing mode) were not infringed. It is hoped that further research would allow even larger reductions in response to be achieved by changes in the model dynamics. Hence if similar or improved methods are applied to other wind tunnel models with realistic aerodynamic characteristics, model responses should be much smaller, and should not endanger the integrity of the balance. A full review of factors affecting model stability made after the initial problem was encountered is given elsewhere(6).

Although the main emphasis is on the problems of testing models in conventional wind tunnels, similar problems could occur when testing models of advanced combat aircraft at high angles of incidence, or without a fin, in cryogenic wind tunnels. Due to the predominance of aerodynamic damping over structural damping<sup>(7)</sup> (as compared to a model in a conventional wind tunnel) any buffeting responses generally will be smaller and therefore less serious. In contrast any flutter responses will be larger and therefore more serious than in a conventional wind tunnel. Hence test engineers in cryogenic facilities should be aware of these recommended changes in model design and test procedure.

## 2 EXPERIMENTAL DETAILS

Fig 4 shows the general arrangement of RAE Model 2209, which has a thin, highly swept wing mounted on top of an almost square fuselage.

### Instrumentation

The model was supported on a 3" diameter strain gauge balance and measurements were made of both the dc and ac components of the strain gauge signals. The dc components were used to compute the static forces and moments, and to ensure that the steady design limits for the balance were not exceeded. The ac components were used to activate audible alarms in the wind tunnel control room, either when the rms level exceeded 20% of the maximum allowable dc level, or when the dc level plus the rms level exceeded the maximum allowable dc level. (The audible alarms corresponded with a model amplitude of about 50 mm in the vertical bending mode and about 0.5° in the horizontal yawing mode.)

The criterion of a rms level 20% of the maximum dc level is based on the normal force fluctuations on rigid aerofoils<sup>(8)</sup> which show maximum rms values of  $C_N = 0.1$  in the presence of a mean  $C_N$  of about 1. However, the normal force fluctuations on rigid wings are generally somewhat smaller than those on rigid aerofoils, so that this criterion is not restrictive. This criterion will not necessarily be adequate if coupled motion, or single-degree-of-freedom flutter occurs. No balance failures have occurred in the RAE 8ft x 8ft Tunnel since the rms measurement system and the audible warning system were introduced in 1985.

During the initial tests at high angles of incidence the balance audible alarms were activated several times due to motions in both the vertical and horizontal planes. In addition, the model was seen to vibrate in the vertical plane on the TV monitor. Hence these tests were abandoned and a series of special vibration measurements were commissioned. Accelerometers were installed on the fuselage in the positions shown in Fig 4 to monitor the motion in both the vertical and horizontal planes. The accelerometer signals were recorded on magnetic tape and analysed on the RAE PRESTO system<sup>(9)</sup>.

### Modes excited

The modes of vibration inferred from the accelerometer measurements are virtually the same wind-off and wind-on, both with respect to

displacements and frequency. The constancy of frequency implies that even at the highest kinetic pressure the aerodynamic stiffness is small compared to the structural stiffness. This represents a useful simplification of a difficult problem.

During the wind-on tests at high angles of incidence, three rigid body modes were excited (Fig 5).

- (a) Sting balance bending in the vertical plane at a frequency  $f = 6.7$  Hz (Fig 5a) which excited an audible alarm,
- (b) sting balance bending in the horizontal plane at a frequency  $f = 6.3$  Hz (Fig 5b), and
- (c) sting balance overtone bending and model yawing in the horizontal plane at a frequency  $f = 13.5$  Hz (Fig 5c) which also excited an audible alarm.

All three modes were reproduced wind-off by an exciter placed about 1 m downstream of the base of the model. In Fig 5 it should be noted that the displacement scales are magnified greatly relative to the vertical and horizontal scale. No displacements were measured along the sting so that this portion of each mode shape is shown with a dashed line and is tentative. All three modes were very lightly damped in still air, only about 0.4% critical damping as derived from the resonance peak.

### Structural modifications

There were two structural modifications. The first modification was a simple passive tuned damper (Fig 6), which increased the structural damping in the sting bending mode in the vertical plane from 0.4% critical to about 1% critical. Due to the limited space within the model and the short time available, it was not possible to select an 'optimum' damper according to well known criteria<sup>(10,11)</sup>. However these criteria were used for guidance. A strain gauge bridge was applied to the cantilever to measure the motion.

The second modification was a pair of lateral bump stops (cf Fig 7) set to a clearance of only 0.63 mm (0.025 in) to limit the model lateral motion at 13.5 Hz. The bump stops were ineffective at  $f = 6.3$  Hz because this mode involves little motion of the model relative to the sting. The bump stops were faced with rubber to provide energy dissipation on impact.

### Test conditions

Tests were planned in the RAE 8ft x 8ft Tunnel over the incidence range from 10° to 37.5° at Mach numbers from  $M = 0.2$  to 0.8, over a wide range of unit Reynolds number. However this was not possible either with the unmodified model or with the structural modifications because of the severity of model vibration at angles of incidence above about  $\alpha = 25^\circ$ . All the tests were made with free transition, despite the adverse effect this was expected to have on the model motion<sup>(5)</sup>. The emphasis here is on the model dynamics rather than on the model aerodynamics and

hence it is appropriate to discuss variations in kinetic pressure rather than Reynolds number.

### 3 RESULTS

A preliminary analysis of a few typical response signals on magnetic tape showed that there was no coherence between any of the three modes excited. Hence the motion in each of the three modes can be considered separately, both for the unmodified model and the modified model. Only a few response measurements are presented: a full report is available<sup>(6)</sup>.

#### 3.1 Sting bending in the vertical plane at $f = 6.7$ Hz

##### Model without damper

Fig 8 shows measurements at  $M = 0.5$  which relate to the sting bending mode at  $f = 6.7$  Hz. Fig 8a shows that the incidence for the onset of large amplitude motions and the sounding of an audible alarm is about  $24$  to  $26^\circ$  almost independent of kinetic pressure. However an important change in the character of the response occurs at a kinetic pressure of about  $12 \text{ kN/m}^2$ . Below this pressure the model motion is bounded and might be tentatively described as large amplitude buffeting. Above this pressure the model motion builds up rapidly, and the audible alarms on the balance are sounded necessitating a rapid reduction of incidence. This motion is best described as flutter, and is probably divergent.

An attempt was made to relate the observed model motions with the aerodynamic force without endangering the balance or activating the audible alarms. Hence response measurements were made at three low kinetic pressures. Fig 8b shows the variation of the heave amplitude with the mean angle of incidence. For all three kinetic pressures, the model response peaks near  $\alpha = 26^\circ$ , where the maximum response occurs at the intermediate kinetic pressure ( $q = 5.0 \text{ kN/m}^2$ ). For this pressure the Reynolds number is only  $R = 1.8 \times 10^6$  and there are probably large areas of transitional flow on the lower surface of the wing. This transitional flow might be expected both to increase the overall buffet excitation and reduce the damping in the heave mode, consistent with the increased response observed<sup>(5)</sup>.

Time-averaged measurements of the lift suggests that the large heave bending motions might be associated with a region of negative lift curve slope. Fig 9 shows the measured variation of lift coefficient,  $C_L$ , with incidence,  $\alpha$ , for a range of kinetic pressures,  $q$ . The lift coefficient first increases linearly (from  $\alpha = 20^\circ$  to about  $25^\circ$ ), then decreases linearly (from  $\alpha = 26^\circ$  to about  $28^\circ$ ) then increases again more slowly (from about  $\alpha = 29$ - $36^\circ$ ).

(The region of negative lift curve slope is more clearly defined in the original measurements than in the subsequent tests, which are more scattered.) Comparing Figs 9 and 8b, the region of negative lift curve slope is associated with the large amplitude model motions.

It is shown elsewhere<sup>(6)</sup> that the region of negative lift curve slope corresponds with negative aerodynamic damping in this mode. The model motion depends on the total damping,  $\zeta$ , the sum of the negative aerodynamic damping and the positive structural damping (known to be very low for the unmodified model). When the estimated total damping is low the nature of the oscillation is such that there is uncertainty as to whether to call the motion flutter or buffeting. In contrast, once the total damping becomes definitely negative (due to the high magnitude of the negative aerodynamic damping at high kinetic pressures) the model motion definitely represents single-degree-of-freedom flutter. This flutter may either be amplitude limited or divergent. It is interesting to note that the largest negative slope occurs for  $q = 5 \text{ kN/m}^2$  and that this corresponds with the largest response in Fig 8b. For the lowest pressure ( $q = 3.7 \text{ kN/m}^2$ ), the lift curve slope actually becomes negative at about  $\alpha = 23^\circ$ . For  $q = 3.7$  and  $5.0 \text{ kN/m}^2$  the lift coefficients above  $\alpha = 30^\circ$  are very scattered and hence are omitted from Fig 9. The scatter is probably caused by hysteresis or switching of the large scale flow separations caused by the large amplitude model motions shown in Fig 8b.

##### Model with damper

The damper only increases the structural damping from 0.4% critical to 1% critical and this increase is achieved only over a small range of heave amplitude. Although the reductions in response achieved are modest, they are sufficient to prove the value of the concept.

Fig 10 compares measurements for  $M = 0.50$  both with and without the damper. Fig 10a (as Fig 3a) shows that the response with the damper is significantly smaller over the complete incidence range from  $24.5$ - $35^\circ$ . However, it is important to notice that the reduction in response is small at  $\alpha = 27^\circ$  where the largest amplitude motions occur. Fig 10b shows that the static lift coefficients are much the same for both conditions, as expected. However, the scatter on the measurements is less with the damper, particularly for  $\alpha > 30^\circ$ .

The comparative measurements shown in Fig 10 are of interest because the changes involved are apparently only structural. There should be no aerodynamic changes in the mean flow because the Mach number and kinetic pressure are the same, but there could be aerodynamic changes due to the changes in model motion. If the heave motions observed were due to low amplitude buffeting, the aerodynamic forcing function, represented by the buffet excitation parameter in the mode, would be the same for motion with and without the damper. The buffet excitation parameter may be calculated according to the relation<sup>(12)</sup>

$$\sqrt{nG(n)} = \frac{2}{\sqrt{\pi}} \frac{m\ddot{z}}{[qS]\zeta} \quad (1)$$

where  $m$  = generalised mass in the mode,

$\ddot{z}$  = rms heave acceleration, (derived from  $z$ )

$S$  = wing area, and

$\zeta$  = total damping in the mode as fraction of the critical damping.

Table 1 lists the total damping values assumed, which are derived from the sum of the wind-off structural damping coefficient ( $g/2$ ) without and with the damper and aerodynamic damping coefficient ( $\gamma$ ) estimated elsewhere<sup>(6)</sup>.

measurements. This peak may occur in a narrow range of incidence in which a large scale separation switches intermittently from one position to another, as the lift curve slope changes sign. This would represent a bi-furcation, best described by catastrophe theory<sup>(1)</sup>. The level of the peak may well be somewhat lower, (say  $\sqrt{nG(n)} = 50 \times 10^{-3}$ ) but the higher level is preferred as possibly affording a further safety margin.

(c) For  $\alpha = 22^\circ$ ,  $\sqrt{nG(n)} = 6 \times 10^{-3}$ . This level is of the same magnitude, but twice as large as that due to heavy wing buffeting in the first bending mode<sup>(12)</sup>.

Table 1

TYPICAL ESTIMATED DAMPINGS  $M = 0.50$ ,  $q = 7.5 \text{ kN/m}^2$

Damper	Structural $g/2$ (% critical)	$\alpha$ (deg)	Aerodynamic $\gamma$ (% critical)	Total $\gamma + g/2$ (% critical)
Without	0.4	22	+0.3	0.7
		28	-0.1	0.3
		32	+0.06	0.46
With	1.0	22	+0.3	1.3
		28	-0.1	0.9
		32	+0.06	1.06

Fig 10c shows that the values of the buffet excitation parameter calculated according to these assumptions are quite different in some places over the incidence range from 20-37°. The differences are often so large that it is unreasonable to attribute them either to errors in response measurement (due to, say, short record lengths) or to large errors in estimated total damping. Where the two curves differ the heave motions can never be regarded as normal, low amplitude buffeting, even in the regions where the calculated aerodynamic damping is positive. In this region the model motion must be altering the buffet excitation. Both curves converge to a common level at  $\alpha = 35^\circ$ , which is indicative of normal buffeting. This is consistent with very large scale flow separations, for which the buffet excitation is unaltered by the model motion.

#### Damping requirements for future models

For a fixed aerodynamic condition ( $M$ ,  $\alpha$ ,  $q$ ) the model aerodynamics can only be assumed independent of the low frequency motion when the buffet excitation parameter (derived according to equation (1)) is independent of the level of damping. A hypothetical curve for this condition is shown dotted in Fig 10c. The three main features of this hypothetical curve are as follows:

- (a) For  $\alpha = 38^\circ$ ,  $\sqrt{nG(n)} = 58 \times 10^{-3}$ , consistent with the measured response.
- (b) For  $\alpha = 27^\circ$ ,  $\sqrt{nG(n)} = 77 \times 10^{-3}$ ; the same as the peaks observed in both sets of

Usually it will not be possible to make comparative measurements for different levels of structural damping, and hence it is important to establish what level would be adequate for the most adverse situation. Within the present test a level of 1% is inadequate (cf Fig 11a). Despite this it was decided to increase the kinetic pressure by a factor of 2 at both  $M = 0.50$  and 0.70. According to calculations<sup>(6)</sup> the total damping should still have remained positive so that large amplitude motions might have been avoided. This expectation was disappointed. Fig 11a shows that large amplitude motions develop, above  $\alpha = 26^\circ$  for  $M = 0.50$  and above  $\alpha = 22^\circ$  for  $M = 0.70$ , despite the 1% structural damping applicable for small amplitudes. Fig 11b suggests that the static lift characteristic for  $M = 0.50$  at the higher pressure is much the same as the lower pressure. Hence scale effects should be fairly small. The apparent anomaly between the predictions and the observations is explained by reference to the large amplitude of the damper mass.

Fig 12 shows that initially the amplitude of the damper mass, determined from the strain gauge signal is directly proportional to the amplitude of the model, as might be expected. However the dissipation of the system is inadequate and the damper mass hits the side of the surrounding cylinder (Fig 6) when the model vertical bending amplitude is only 38 mm, well below the amplitude, 50 mm, at which the audible alarm sounds. The inadequate dissipation is partially due to the use of a circular mass<sup>(6)</sup>. Once the damper mass hits the cylinder, the model motion increases rapidly. Probably the impact of

the mass on the cylinder provides additional forced motion, possibly in conjunction with reduced structural damping. This is a potentially dangerous situation, which allowed an amplitude of  $z = 66$  mm to be reached at  $M = 0.70$ ,  $q = 15.8$  kN/m<sup>2</sup> at  $\alpha = 26.2^\circ$  before the incidence was reduced.

Thus while Fig 10a shows that the internal damper makes a significant reduction in the heave response, it is apparent from Figs 11 and 12 that much larger increases in damping are required to ensure the safety of this model and future models, particularly at high angles of incidence. This high level of damping must be maintained for high amplitude motions.

### 3.2 Sting bending in the horizontal plane at $f = 6.3$ Hz

The audible alarms were never activated for the motion in this mode because the amplitudes were small (less than 15 mm). The bump stops have no effect because in the sideslip mode there is virtually no relative motion between the end of the fuselage and the sting. Also as the damper provided no damping in the lateral plane no reduction in response was obtained relative to the original configuration. According to quasi-steady theory the aerodynamic damping in this mode was always positive although small<sup>(6)</sup> thus ruling out single-degree-of-freedom flutter.

### 3.3 Sting overtone bending and model yawing at 13.5 Hz

For the unmodified model an audible alarm was activated frequently by yawing oscillations because the amplitudes required were only about  $0.5^\circ$ .

Fig 13 shows all the measurements made of the variation of amplitude with angle of incidence and speed. For  $M = 0.50$  and varying kinetic pressures (Fig 13a) the amplitude increases monotonically with the angle of incidence, but has no consistent variation with kinetic pressure. For  $q = 7.5$  kN/m<sup>2</sup> the audible alarm for this mode is activated at  $\alpha = 37^\circ$ . It is significant that this occurs well above the incidence range ( $\alpha = 26-29^\circ$ ) for large amplitude motions in the heave mode (cf Fig 8). This implies that the phenomena exciting the motions are different, consistent with the lack of coherence between the modes already noticed.

Fig 13b shows a collection of measurements for widely varying speeds. For  $q = 7.5$  kN/m<sup>2</sup>, there is a somewhat smaller response at  $M = 0.60$  and  $0.70$  than at  $M = 0.50$ . This would be consistent with the inference made elsewhere<sup>(6)</sup> that the vortex configurations exciting the motions are strongest at the lowest Mach number and decrease in effectiveness as Mach number increases. The relatively high level of response in the range from  $\alpha = 30-33^\circ$  at  $M = 0.25$ ,  $q = 5.8$  kN/m<sup>2</sup> (the lowest value) should be noted. Possibly this high level of response indicates heavy buffeting, above the region of vertical bending in the incidence range from  $\alpha = 26-29^\circ$ . Fig 13b shows also that for  $M = 0.70$ ,  $q = 15.8$  kN/m<sup>2</sup> the audible alarm was not activated for the yawing mode despite the activation of the audible alarm for the vertical

bending mode (cf Fig 11a). This difference is consistent with the lack of coherence between the two modes.

Fig 13c (as Fig 3b) shows the influence of the bump stops at  $M = 0.50$ ,  $q = 7.5$  kN/m<sup>2</sup>. When the angle of incidence increases above about  $\alpha = 35^\circ$ , lateral motions develop causing the sting to make contact with the rubber surface of the bump stops. Then further increases in amplitude with incidence are prevented and the apparent damping in the mode (inferred from the spectra) increases from about 1% critical to 4% critical: this increase is due to the energy dissipated during the impact. Hence with the bump stops the model amplitude never becomes sufficiently large to activate the audible alarm system. The bump stops are effective because in the yawing mode there is relative motion between the end of the fuselage and the sting.

Manifestly, the bump stops represent a useful 'fail-safe' feature of the interim modification because they prevent large amplitude yawing motion and safeguard the balance from failure in this mode. However, they do not allow reliable measurements to be made at high angles of incidence because the model is still in motion. Ideally higher levels of damping should be provided for the amplitude range from  $0-0.4^\circ$ , so that the bump stops are never encountered during routine tests.

For a body without a fin, although the aerodynamic damping in the yawing mode may be positive at low angles of incidence, it often becomes negative at high angles of incidence, due to the formation of asymmetric vortices. Currently it is not possible to predict the damping in this mode theoretically, or even to infer it approximately from quasi-steady measurements. Thus the possibility of large amplitude single-degree-of-freedom flutter cannot be excluded and there is some evidence for this condition within the measurements<sup>(6)</sup>.

## 4 DISCUSSION

The dynamic problem experienced on this model is now discussed in a broader context. The problem is caused by the new requirement to test simultaneously at high angles of incidence (say  $25-35^\circ$ ) and high kinetic pressures, to establish the magnitude of scale effects when there are large regions of separated flow. Under these conditions severe buffeting and/or single-degree-of-freedom flutter can occur, at low frequency, rigid body modes of the model associated with sting vibrations. The responses may become sufficiently large to endanger the balance, quite apart from vitiating the static measurements. The only solution to the problem using existing balances is to provide much higher total dampings in these modes by increasing the structural damping. An alternative, much less attractive, long-term solution would be to develop a new generation of balance/stings, which have high internal damping and greater stiffness. This solution and other palliatives which might alleviate the vibrations are discussed elsewhere<sup>(6)</sup>.

A severe test was required because models of a specific combat aircraft might have sudden, adverse changes in aerodynamic characteristics. Such changes could be due to variations with Reynolds number (even with fixed transition) or to variations in Mach number, particularly at transonic speeds. As an example, configurations with fins which lose lateral stability at high angles of incidence are likely to have negative aerodynamic damping in the horizontal bending or sideslip mode and single-degree-of-freedom flutter could occur. If single-degree-of-freedom flutter occurred simultaneously in both the horizontal and vertical bending modes, probably the consequences would be catastrophic. The present measurements provide useful criteria for the structural damping coefficients required for model safety at high angles of incidence.

Fig 14 shows that to prevent single-degree-of-freedom flutter at  $M = 0.50$ , and  $p_t = 4$  bar, structural damping must be in the range from  $g/2 = 2\%$  to  $4\%$  critical damping. The upper limit would allow the normal force curve slope to be  $-3.2$  (ie twice that of the present measurements). Fig 14 shows also that to limit the heavy buffeting at high angles of incidence, structural damping must be in the range from  $g/2 = 4\%$  to  $6\%$ . Here the upper limit allows the maximum buffet excitation parameter at  $\alpha = 28^\circ$  to be  $\sqrt{nG(n)} = 77 \times 10^{-3}$  (from the hypothetical curve) and the negative normal force curve slope to be increased to  $-3.2$ . Compared to both of these criteria, the damping of the unmodified model is totally inadequate, only about  $g/2 = 0.4\%$ . This low value is typical of most sting mounted models tested in the RAE 8ft  $\times$  8ft Tunnel.

The addition of the tuned viscous damper only increased the structural damping from  $g/2 = 0.4\%$  to  $1\%$ , compared to the level  $g/2 = 3.5\%$  achieved previously<sup>(5)</sup>. There the generalised mass in the wing first bending mode was much smaller, so that the mass ratio was appreciably higher, allowing a higher dissipation<sup>(10,11)</sup>. With a tungsten mass of optimum shape, damping levels can be maintained over a wider range of amplitude<sup>(6)</sup>. Plainly  $1\%$  damping is too low, and further increases must be obtained.

Two different possibilities are being considered. The first is to replace the steel spring of the cantilever in Fig 6 (which has low internal damping) with a composite cantilever (having high internal damping). Such an arrangement would be much more effective, and less sensitive to small changes in frequency than the spring steel cantilever with low internal damping. The internal damping provided by the new cantilever might even be sufficiently high to obviate the need for viscous dissipation, provided by oil. Such a damper would be easier to install. Levels of damping of  $g/2 = 1\%$  to  $3\%$  can be achieved by this means. The second possibility would be to provide the sting with a shroud. It is possible that levels of damping from say,  $g/2 = 2\%$  to  $6\%$ , might be achieved by a sting shroud particularly for the first harmonic mode, which involves appreciable sting motion (see Fig 5c). Combining both these possibilities, levels of structural damping in the range from  $g/2 = 3\%$  to  $9\%$  might be achieved.

These levels would suffice to prevent single-degree-of-freedom flutter (the dangerous condition) and also should be adequate to limit heavy buffeting when the aerodynamic damping is small.

In a cryogenic wind tunnel somewhat higher levels of structural damping are required (say  $g/2 = 7\%$  to  $10\%$ ) as compared to a conventional wind tunnel. This is because of the increased magnitude of any negative aerodynamic damping relative to structural damping at cryogenic temperatures<sup>(7)</sup>. In a cryogenic tunnel at constant Mach number, if Reynolds number is increased at constant total pressure and kinetic pressure by lowering the total temperature, the velocity decreases according to the relation

$$U \propto M\sqrt{T_t} \quad (2)$$

thus increasing the frequency parameter. For a given model with fixed structural frequencies the increase in frequency parameter is associated with an increased magnitude of the aerodynamic damping according to the relation

$$\rho U \propto \frac{M p_t}{\sqrt{T_t}} \quad (3)$$

because the effect of the decrease in velocity is overcome by the effect of the increase in free-stream density. The damping coefficient (which could be positive or negative) could modify the type of vibrations observed on a particular model as between cryogenic and ambient conditions. Hence model dynamics at high angles of incidence may be more critical in cryogenic wind tunnels than in conventional tunnels. If the total temperature is lowered from  $300$  to  $100$  K, the aerodynamic damping according to equation (3) is increased by a factor of  $\sqrt{3} = 1.7$ . Hence the higher levels of structural damping suggested above are thought necessary.

Even when high levels of structural damping are achieved in sting modes, bump stops should be provided as a further safeguard, both against oscillations of large amplitude as well as against excessive static moments. However bump stops can only be effective when there is relative motion between the model and the sting (as for the yawing mode at  $13.5$  Hz here) or for pure pitching and yawing motions on the balance. Whether or not high levels of structural damping are provided, bump stops provide a simple safeguard for some modes and should be included as a matter of routine.

5 CONCLUSIONS

Some brief tests of Model 2209 in the RAE 8ft x 8ft Tunnel suggest four main conclusions relevant to model dynamics.

- (1) Wind tunnel models with lightly damped, support modes ( $g/2 = 0.4\%$ ) are likely to vibrate at high angles of incidence and high kinetic pressures. Special precautions should therefore be taken when designing such models and planning the order of the test programme.
- (2) The vibrations observed may be due to buffeting or to single-degree-of-freedom flutter. In either case a structural damping coefficient of between 4% and 6% should suffice to exclude unacceptable amplitudes in a conventional wind tunnel. In a cryogenic tunnel somewhat higher levels are required, say  $g/2 = 7\%$  to 10%.
- (3) Bump stops provide a simple and effective safety device for balances, both with respect to static and dynamic loads, and should be fitted as a matter of routine.
- (4) Research is needed to develop an effective shroud damper for sting supported models. Such a damper would provide a large increase in damping for all sting modes, independent of amplitude. If a shroud damper can be developed giving  $g/2 = 4\%$  to 6%, internal dampers would only be required for balance modes involving no sting motion. [Balance modes might be damped by bump stops.]

LIST OF SYMBOLS

$C_L, C_m$	lift and pitching moment coefficients
$C_N$	normal force coefficient
$\bar{c}$	aerodynamic mean chord of wing (0.483 m)
$f$	frequency (Hz)
$g/2$	structural damping coefficient (fraction of critical)
$M$	Mach number
$m$	generalised mass
$\sqrt{nG(n)}$	buffet excitation parameter (equation 1)
$p_t$	total pressure (bar)
$q = \frac{1}{2}\rho U^2$	kinetic pressure (N/m <sup>2</sup> )
$U$	free stream velocity (m/s)
$R$	Reynolds number based on $\bar{c}$
$S$	wing area (0.400 m <sup>2</sup> )
$T_t$	total temperature (K)
$\ddot{z}$	acceleration of model centre of gravity

$\alpha$	angle of incidence
$\beta$	angle of sideslip
$\bar{\beta}$	rms angle of sideslip
$\gamma$	aerodynamic damping coefficient (fraction of critical)
$\nu = 2\pi f \bar{c} / U$	frequency parameter
$\zeta = \gamma + g/2$	total damping coefficient (fraction of critical)

REFERENCES

- (1) J.G. Jones, Dynamic response of aircraft with fluctuating flow fields in "Unsteady airloads and aeroelastic problems in separated and transonic flow". VKI Lecture Series, (1981-4)
- (2) D.G. Mabey, Beyond the buffet boundary. Aeronautical Journal, (1973)
- (3) D.G. Mabey, Flow unsteadiness and model vibration in wind tunnels at subsonic and transonic speeds. CP 1155, (1971)
- (4) J.W.G. van Nunen Notes concerning testing time requirements in steady and unsteady measurements. Paper 2, AGARD R615, (1974)
- (5) D.G. Mabey, P.R. Ashill, B.L. Welsh, Aeroelastic oscillations caused by transitional boundary layers and their attenuation. AIAA J. Aircraft, Vol 24, No.7 pp 463-469, (1987)
- (6) D.G. Mabey, B.L. Welsh, C.R. Pyne, The reduction of rigid-body response of sting supported models at high angles of incidence. RAE Technical Report TR 89-012, (1989)
- (7) D.G. Mabey, Some remarks on dynamic aeroelastic model tests in cryogenic wind tunnels. NASA CR 145029, (1975)
- (8) P.P. Polentz, W.A. Page, L.L. Levy, The unsteady normal force characteristics of selected NACA profiles at high subsonic Mach numbers. NACA RM A65 C02, NACA T1B 4683, (1955)
- (9) B.L. Welsh, D.M. McOwat, Presto: a system for the measurement and analysis of time dependent signals. RAE Technical Report 77155, (1977)
- (10) S. Timoshenko, D.H. Young, Advanced dynamics. Chapter A, Art 37, McGraw Hill, New York, (1948)
- (11) J.P. Den Hartog, Mechanical vibration. McGraw Hill, New York, (1956)
- (12) D.G. Mabey, Some aspects of aircraft dynamic loads due to flow separation. AGARD Report R750 (1987), or Prog Aerospace Sci Vol 26, pp 115-151, (1989)

Copyright © Controller HMSO London 1990  
Published by the American Institute of Aeronautics and Astronautics, Inc. with permission.

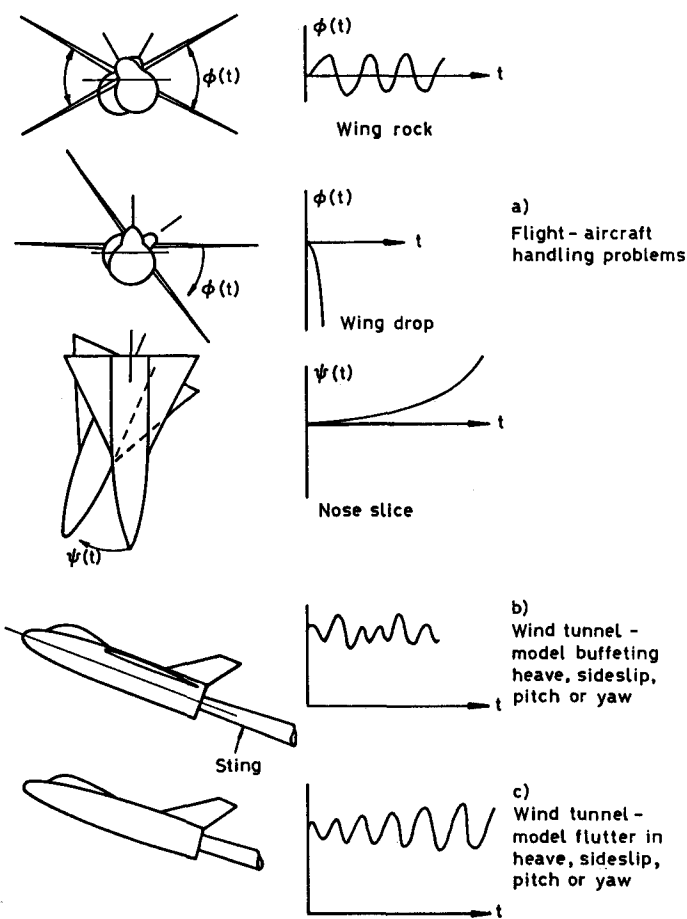


Fig 1 Rigid body motions at high angles of incidence

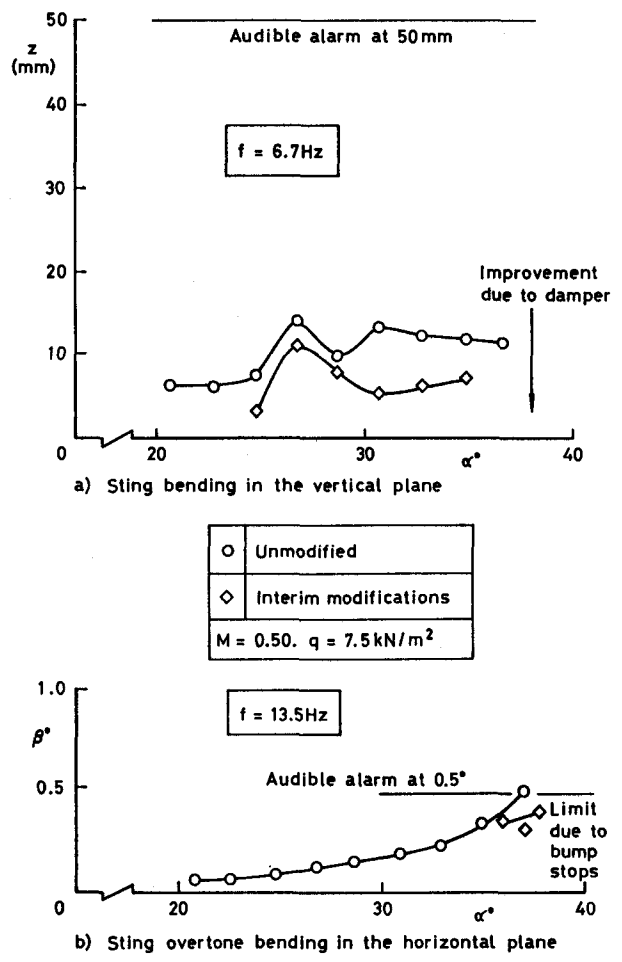


Fig 3 Typical reductions in response due to interim structural modifications

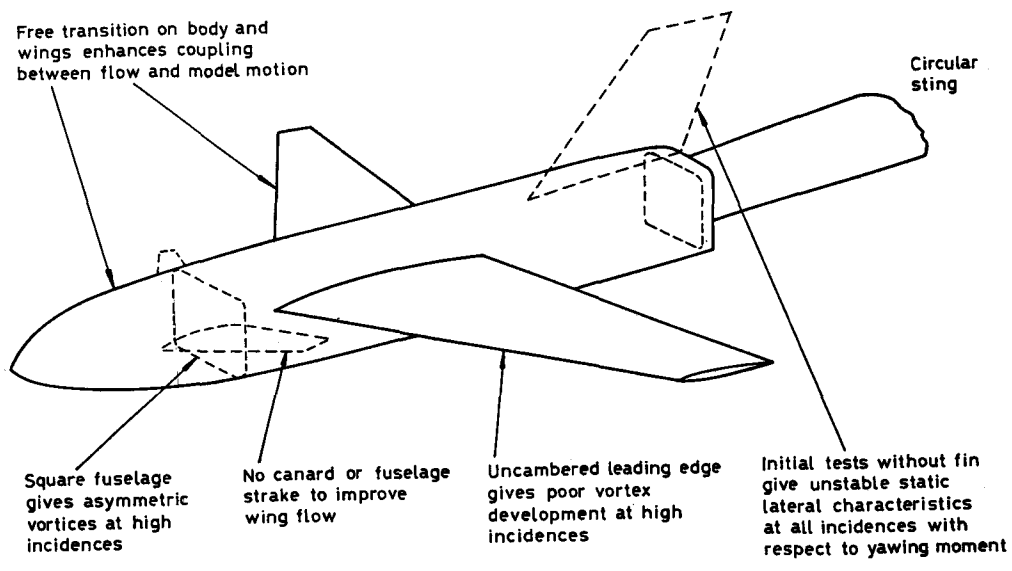


Fig 2 Adverse geometric features of RAE Model 2209



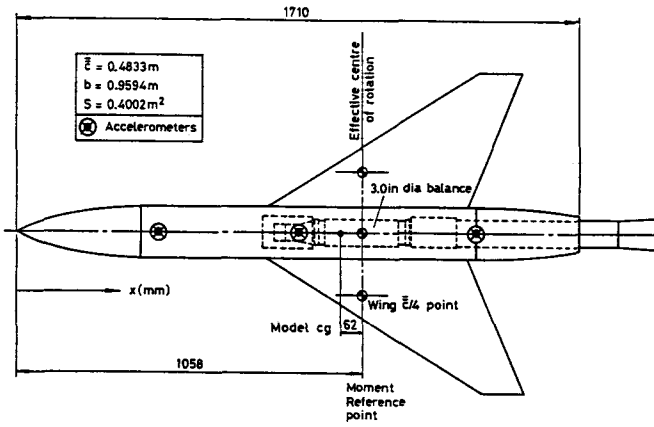


Fig 4 RAE Model 2209

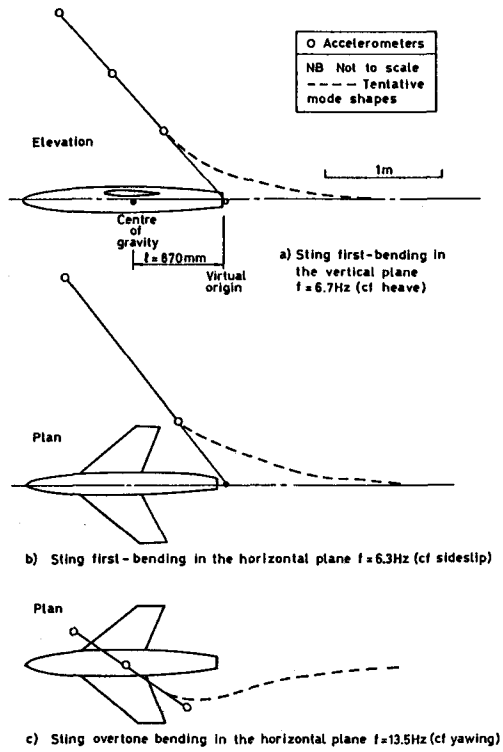


Fig 5 Modes excited wind off and wind on

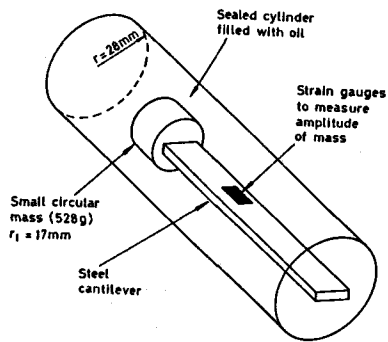
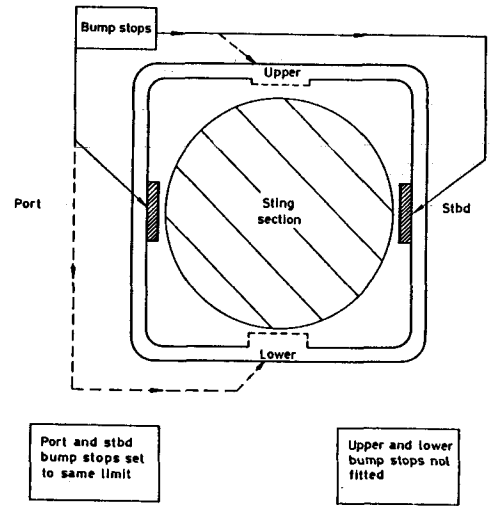
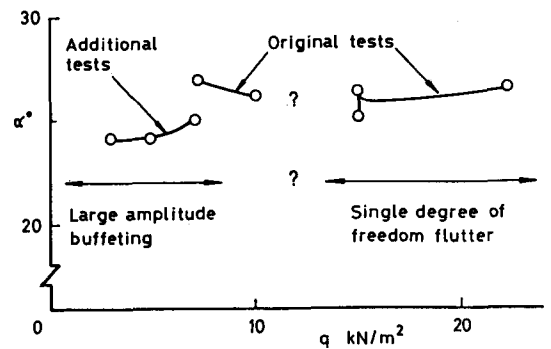


Fig 6 Passive tuned damper

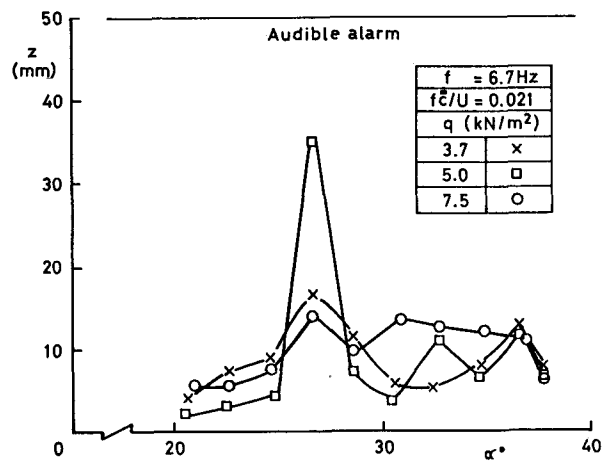


View of model base looking upstream

Fig 7 General arrangement of bump stops

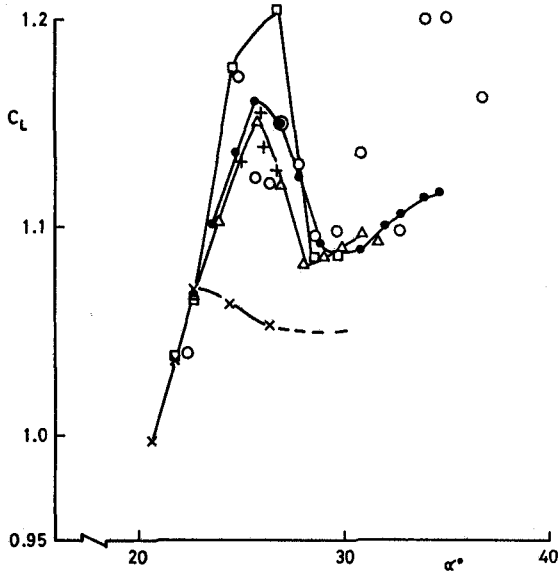


a) Variation of angle of incidence for audible alarm with kinetic pressure



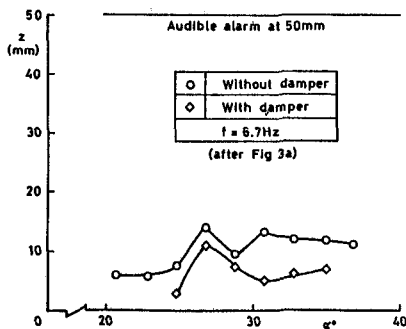
b) Variation of amplitude with incidence

Fig 8 Sting bending in the vertical plane at  $f = 6.7\text{ Hz}$  for  $M = 0.50$  and varying kinetic pressures

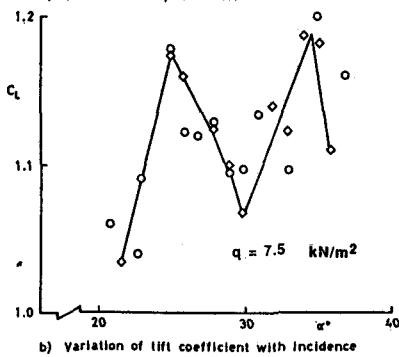


Tests	q (kN/m <sup>2</sup> )	Symbol	R x 10 <sup>-6</sup>
Present	3.7	x	1.2
	5.0	□	1.8
	7.5	○	2.4
Original	7.5	●	2.4
	10.0	△	3.2
	15.0	+	4.8

Fig 9 Variation of lift coefficient with incidence for varying kinetic pressure

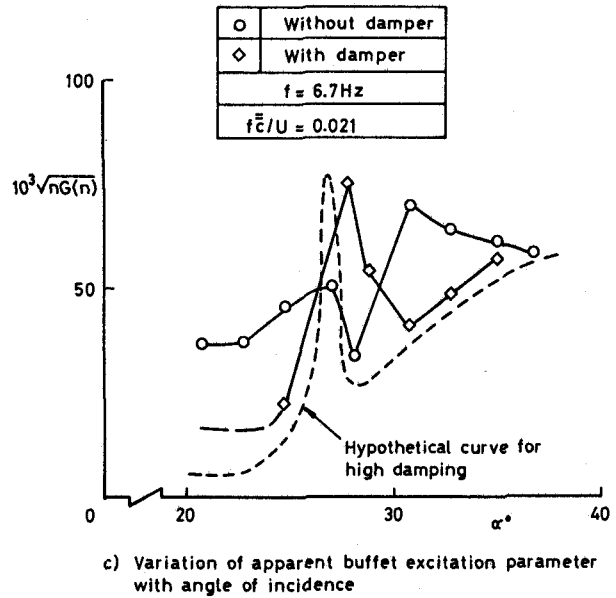


a) Variation of amplitude with incidence



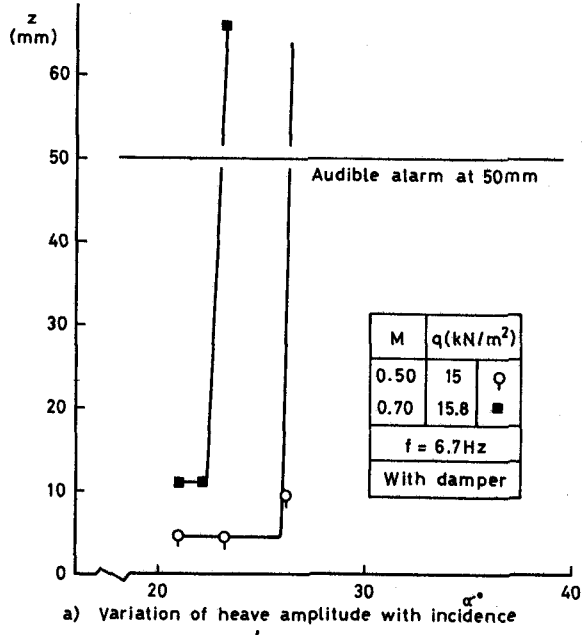
b) Variation of lift coefficient with incidence

Fig 10 Effect of damper on sting bending at  $f = 6.7$  Hz for  $M = 0.50$ ,  $q = 7.5$  kN/m<sup>2</sup>

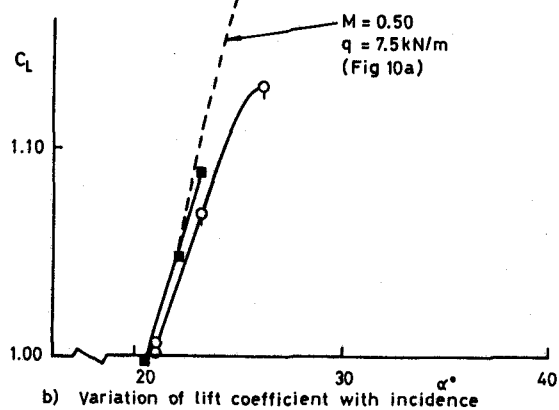


c) Variation of apparent buffet excitation parameter with angle of incidence

Fig 10 (concluded) Effect of damper on sting bending at 6.7 Hz for  $M = 0.50$ ,  $q = 7.5$  kN/m<sup>2</sup>



a) Variation of heave amplitude with incidence



b) Variation of lift coefficient with incidence

Fig 11 Modified model - motion in vertical bending mode for  $M = 0.50$  and  $0.70$  for higher kinetic pressure

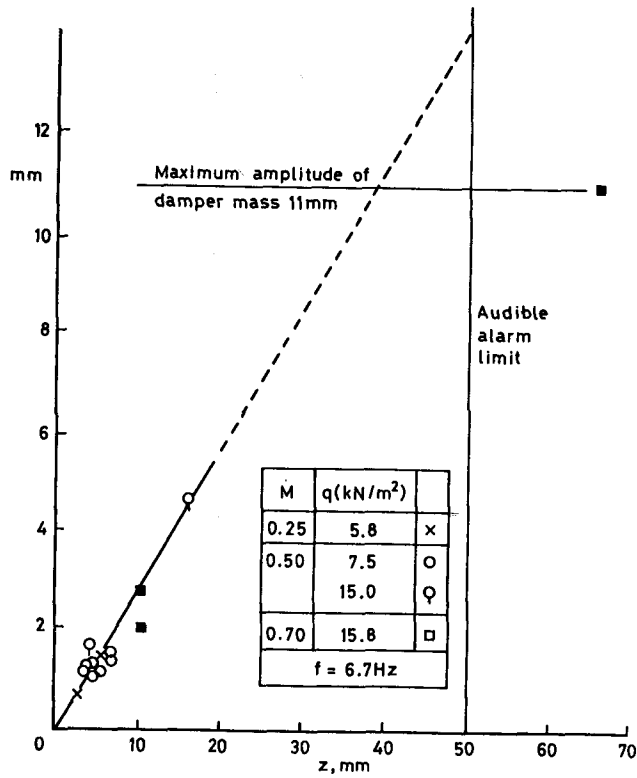
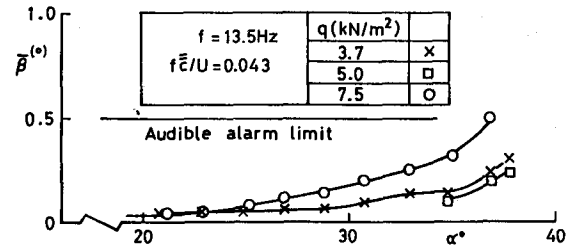
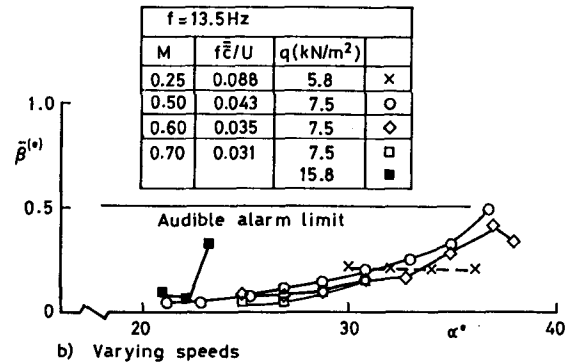


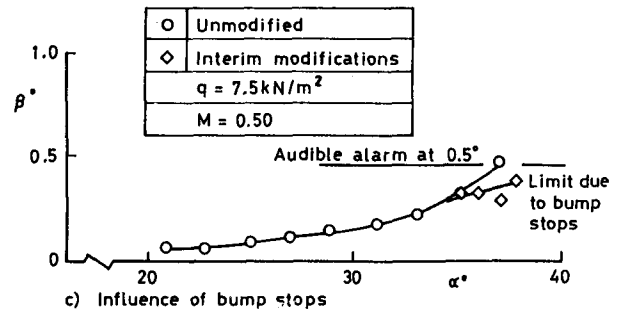
Fig 12 Variation of amplitude of motion of damper mass with model vertical bending amplitude



a) M = 0.50, varying kinetic pressures



b) Varying speeds



c) Influence of bump stops

Fig 13 Variation of amplitude in yawing mode with angle of incidence (zero mean sideslip)

g/2 (% critical)	Criteria for structural damping	Model configurations				
		Unmodified	Present tuned viscous damper	Proposed tuned damper	Sting shroud	Tuned damper + shroud
10						
5	To limit buffeting at high $\alpha$					?
2	To prevent single-degree of freedom flutter		o Ref 5	?	?	?
1			Tungsten mass ?			
1			x Present tests			
0.5			x Present tests			
0.2	Mode(s) frequencies		Single vertical bending		All	All

Fig 14 Structural damping required for model safety at high angles of incidence,

M = 0.50 , p<sub>t</sub> = 4 bar , T<sub>t</sub> = 300 K